Single photon beat note in an acousto-optic modulator-based interferometer

Renaud Mathevet, Benoît Chalopin, Sébastien Massenot

Single photon beat note in an acousto-optic modulator-based interferometer

Renaud Mathevet

Laboratoire National des Champs Magnétiques Intenses,

UPR3228 CNRS/INSA/UJF/UPS, Toulouse, France

Benoit Chalopin

Université de Toulouse, UPS, Laboratoire Collisions Agrégats Réactivité,

IRSAMC; F-31062 Toulouse, France and

CNRS, UMR 5589, F-31062 Toulouse, France

Sébastien Massenot

ISAE-SUPAERO, Université de Toulouse, France

(Dated: September 17, 2019)

Abstract

We present in the following a quantum optics experiment appropriate for advanced undergraduate students with former experience in quantum optics. It extends classical single photon setups to the time dependent domain. We demonstrate self-heterodyning of heralded single photons using a Mach-Zender like interferometer where beamsplitters are replaced by two acousto-optic modulators (AOMs). The single photon beat note is recorded over time at the frequency difference between the RF generators driving the AOMs, which makes it observable directly on a human time scale *i. e.* with periods above a fraction of a second. To compare with our observations, we tailor the standard quantum optics formalism for beam splitters to take into account the frequency shifts associated with the AOMs.

I. INTRODUCTION

Experimental demonstrations can greatly enhance the learning curve in quantum physics, as it complements the usual theoretical approach of a very abstract and non-intuitive topic. The wave-particle duality is very often illustrated with an interference buildup with single photons or single electrons in an interferometer (see for instance [1, 2] for electrons and [3, 4] for photons). In these experiments, the wave is split spatially into two parts, and the recombination forms the interference pattern, that appears over time as events recorded one at a time. This shows that a photon or electron do interfere with itself.

Quantum optics experimental demonstrations for undergraduate or graduate students have become available in the early 2000's owing to technological developments [5, 6]. They are nowadays widespread and we refer to [7] for a quite comprehensive review. Single photon interferences with a Mach-Zenhder interferometer and a spontaneous parametric down-conversion source is one the most popular experiment. We extend on this classical setup replacing the beam splitters by acousto-optic modulators (AOMs). Each of them shifts the reflected beam by a tunable frequency. As a consequence we produce single photon Fock states associated with an unusual bichromatic field mode. Such single photons are thus in a non-stationary state and exhibit periodic oscillations in both time and space termed beat note. Contrary to a previous realization [8], our apparatus allows arbitrary small frequency difference between the two field components. It allows direct observation of beat notes with the roll mode of an oscilloscope. Moreover, most of demonstration experiments deal with the spatial or polarization degrees of freedom of single photon state. Here, we manipulate optical frequencies which widens the range of controllable optical fields observable (see for instance [9]). Naturally, our setup is intended for students already trained in experimental quantum optics as an introduction to advanced concepts such as quantum coherence.

This article is organized as follows. We first quickly present how AOMs may be used as beam splitters and introduce an original matrix approach to describe the different modes involved in the interferometer. We then depict the experimental setup before we discuss our main results. A more detailed analysis of quantum beam splitters and AOMs as well as extra experimental data are postponed in a separate Supplementary Information [URL will be inserted by AIP].

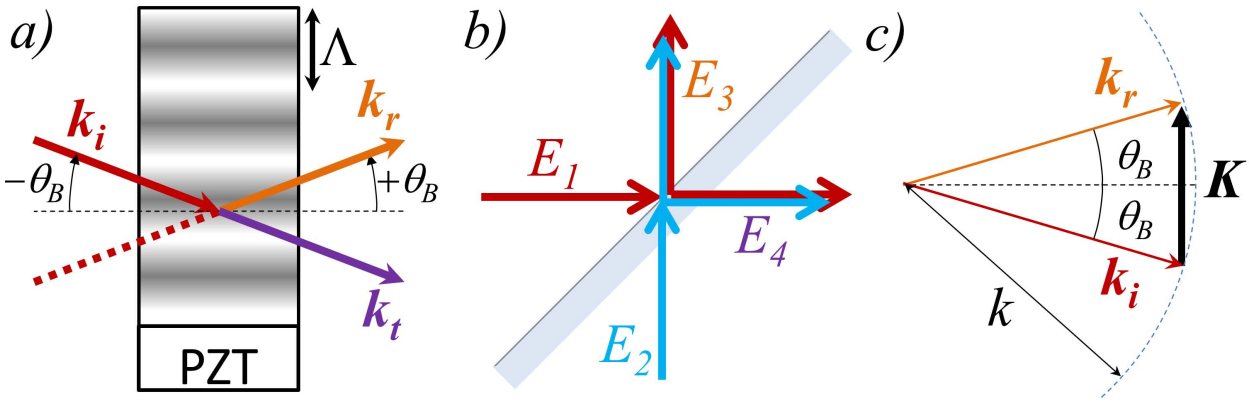

FIG. 1. (Color online) AOMs as beam splitters. $\mathbf{k}_{i,t,r}$ represent light wavevectors of common modulus k. $\mathbf{K}$ is the acoustic wavevector. a) sketch of an AOM. An incoming light beam (red) at Bragg incidence θ_B is partially reflected (orange) and transmitted (purple) by diffraction on an acoustic wave of wavelength Λ generated by a piezoelctric transducer (PZT). A similar process occurs at symmetric incidence (red dotted line). b) E_{1-4} are the field modes impinging on and emerging from a usual optical beam splitter c) Bragg diffraction interpreted as energy and momentum conservation of an incoming photon absorbing a phonon of the acoustic wave.

II. AOMs AS BEAM SPLITTERS

In an AOM, a piezoelectric transducer generates an acoustic wave of angular frequency Ω in a transparent medium (Fig. 1a). It creates a periodic perturbation of the refractive index through the photoelastic effect that propagates at the sound velocity v_s. The medium behaves as a thick grating of spatial period Λ and wavevector $K = 2\pi/\Lambda = \Omega/v_s$, leading to Bragg diffraction of an incident optical wave. Since the grating is time-dependent, optical wavelength is slightly modified during the process.

In the context of a quantum optics experiment, we adopt here a complementary corpuscular point of view to derive the Bragg condition: AOMs can be thought as coherent sources of phonons of energy $\hbar\Omega$ and momentum $\hbar\mathbf{K}$. Incoming photons of energy $\hbar\omega_i$ and momentum $\hbar\mathbf{k}_i$ may absorb or emit a stimulated phonon. Energy and momentum conservation put the following constraints on the reflected photon energy $\hbar\omega_r$ and momentum $\hbar\mathbf{k}_r$:

$$\hbar\mathbf{k_r} = \hbar\mathbf{k}_i \pm \hbar\mathbf{K} \quad \text{and} \quad \hbar\omega_r = \hbar\omega_i \pm \hbar\Omega, \tag{1}$$

where the $+$ and $-$ sign hold for absorption and emission processes.

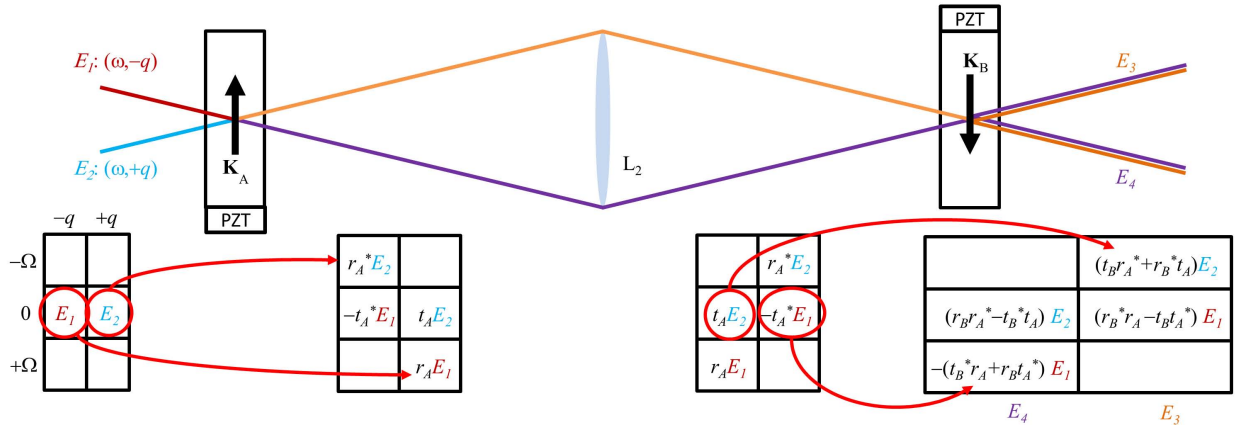

FIG. 2. (Color online) Upper part: simplified scheme of our interferometer with 2 AOMs as beam splitters. The lens L_2 conjugates the beam waist in the first AOM into the second AOM in a $2f - 2f$ configuration. Lower part: matrices representing the propagation of the amplitudes of the different modes in angular frequency $(-\Omega, 0, \Omega)$ and transverse momentum $(-q, +q)$ with $q = K/2$. Red arrows outline the reflection processes in each AOM which depend on the direction of propagation the acoustic wave (black arrows). In practice light is actually sent from only one input ($E_2 \equiv 0$). From a quantum optics point of view single photons are injected at port 1 and vacuum at port 2. The input field state is thus $|\psi\rangle = |1\rangle_1|0\rangle_2$.

For typical AOMs, $v_s \approx 4$ km.s^{-1} so $\Lambda \approx 60$ μm at $\Omega/2\pi \approx 70$ MHz. The wavelength of the photons is $\lambda = 2\pi c/\omega \approx 810$ nm therefore $K \ll k_i$. Then:

$$|\mathbf{k}_r|^2 = |\mathbf{k}_i|^2 \pm 2\mathbf{k}_i.\mathbf{K} + |\mathbf{K}|^2 \simeq |\mathbf{k}_i|^2. \tag{2}$$

Let us decompose the incident wavevector $\mathbf{k}_i = \mathbf{k}_\parallel + \mathbf{k}_\perp$ into its parallel and perpendicular components with respect to $\mathbf{K}$. Eq. 2 then reads $\mathbf{k}_\parallel \simeq \mp\mathbf{K}/2$. We have thus:

$$\mathbf{k}_i = \mathbf{k}_\perp \mp \mathbf{K}/2 \quad \text{and} \quad \mathbf{k}_r \simeq \mathbf{k}_\perp \pm \mathbf{K}/2. \tag{3}$$

The incident and reflected beams propagate symmetrically at angles $\pm\theta_B$ from the axis with $\sin\theta_B = K/2k$ (Bragg condition). A rigorous treatment is derived in the supplementary material.

We have thus a simple picture of an AOM acting as a beam splitter. The two symmetric output ports correspond to hermitian conjugate processes of phonon emission and absorption which results in opposite momentum transfers and frequency shifts on the incoming photons (Fig. 1c).

III. BEAM SPLITTER MATRIX GENERALIZATION

For a usual optical beam splitter the input and output field states are represented by the vectors $(E_1, E_2)^\intercal$ and $(E_3, E_4)^\intercal$. The linear relationships between them are conveniently expressed in matrix form as [10, 11]:

$$\begin{bmatrix} E_3 \\ E_4 \end{bmatrix} = \begin{bmatrix} r & -t^* \\ t & r^* \end{bmatrix} \begin{bmatrix} E_1 \\ E_2 \end{bmatrix} = U \begin{bmatrix} E_1 \\ E_2 \end{bmatrix}. \tag{4}$$

In order to confirm that AOMs can be considered as beam splitters, we give in the Supplementary Material [URL will be inserted by AIP] a classical derivation of the *beam splitter matrix* U and a wave approach of AOMs theory to show that they are actually properly described by such a matrix and identify the relevant phases. We take $r = -ir_{max}e^{-i\Omega t}$ and $t = \sqrt{1-|r|^2}$.

For AOMs operated at Bragg angle we saw before that beams have only two possible transverse wavevectors $\pm K/2 = \pm q$. Reflection is associated to an angular frequency change $\pm\Omega$ while the transmitted beam remains at the same frequency. The field states are thus represented by a 3×2 *mode matrix* containing the amplitudes of its $(-\Omega, 0, +\Omega) \times (-q, +q)$ components (Fig. 2-bottom left).

Interaction with an AOM consists in amplitude redistribution among these 6 components. In principle, the beam splitter matrix can be replaced by a 4-rank tensor. However, it is a large object, hard to visualise, with $3^2 \times 2^2 = 36$ coefficients which however only 4 are non zero. In practice, simple sketches like the red arrows depicted in Fig. 2 are more intuitive and easily implemented in computer algebra. Notice that if the acoustic wave propagates downwards $\mathbf{K} \to -\mathbf{K}$ momentum exchanges are reversed, and so do the red arrows.

The use of one such AOM as a beam splitter is a conventional technique known as *heterodyning* to improve signal-to-noise ratio in interferometric metrology [12]. The meaningful phase information is indeed translated to RF/HF frequencies where technical noise is greatly reduced. However, in the context of quantum optics, it complicates significantly data acquisition [8] as the single photon rate is usually (much) lower than the AOM's modulation frequency *i.e.* we have (much) less than a photon per period.

For demonstrative and pedagogical purposes we have independently developed a double heterodyning scheme where two AOMs are used to shift the signal up and back to low frequencies enough so that the beat note can be real-time recorded with a convincing signal-to-noise ratio on an oscilloscope.

IV. EXPERIMENTAL SETUP

Our experimental setup is depicted in Fig. 3. It consists in essentially three parts outlined by color boxes. We use a conventional single photon source (red box) based on spontaneous

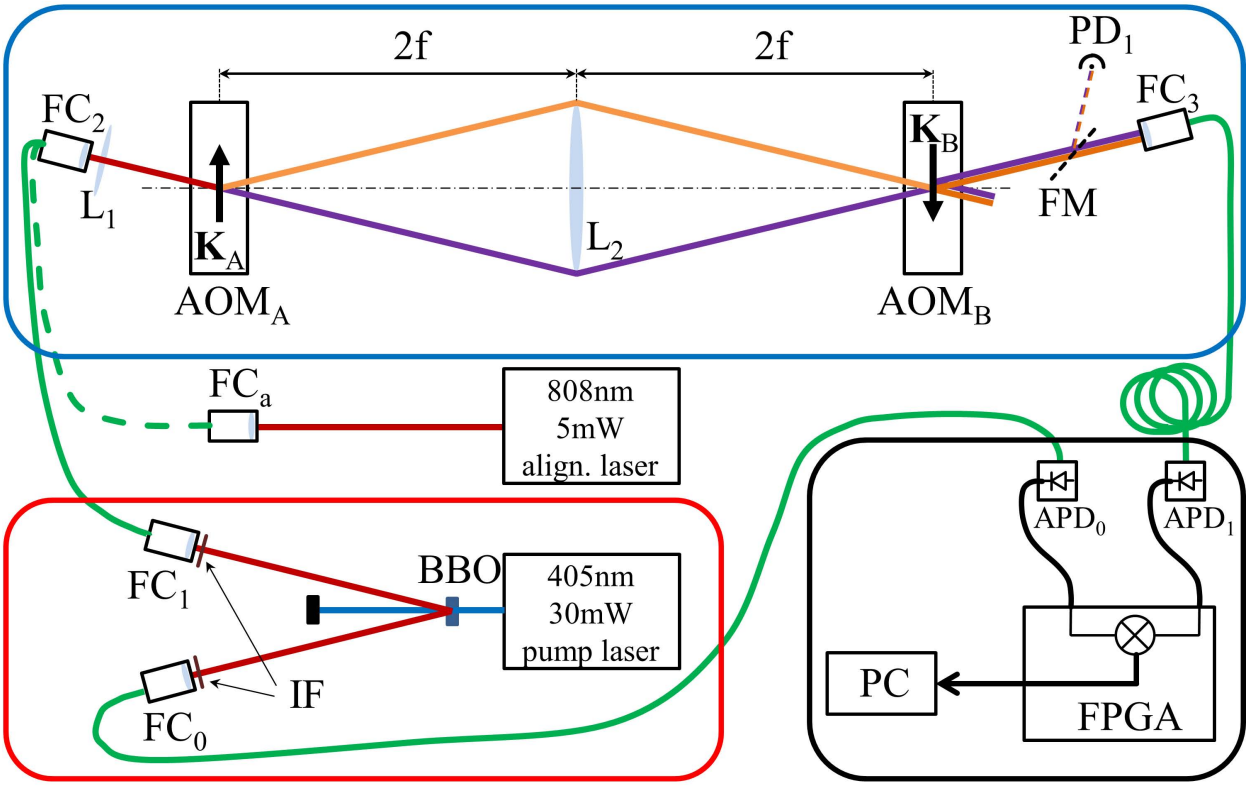

FIG. 3. (Color online) The experimental setup is made of a single photon source (red box), a detection module (black box) and the interferometer (blue box). The meaning of the different labels is L: lens, FC: fiber coupler, APD: avalanche photodiode, IF: interference filter, FPGA: field programable gate array, PC: personal computer. Green lines represent multimode fibers. For alignment purposes and classical light operation we use an extra fiber-coupled (green dashed line) 808 nm laser. A flip mirror (FM) is lifted and light directed on conventional linear photodiodes (PD).

parametric down conversion [5, 6, 13, 14]. A 30 mW, 405 nm laser diode pumps a 1 mm-long crystal of beta-barium borate (BBO) producing photon pairs, whose wavelengths are both centered at 810 nm via type-I down-conversion. Crystal orientation is such that photons are emitted in separate directions $\sim 3^\circ$ apart from the pump laser direction. 50 cm downstream, beams are separated enough to be injected into multimode fibers after passing a 10 nm bandwidth interference filter.

Down-converted photons are produced simultaneously. One photon, labeled by a subscript 0, is directly sent into a 5m-long multimode fiber connected to an avalanche photodiode that triggers the coincidence detection module. It heralds the presence of the second photon which is directed towards the interferometer with a 2m-long multimode fiber.

The detection module (black box) consists in several single photon detectors based on silicon avalanche photodiodes (APD_{0-1}) connected to a FPGA card (Altera DE2-115). This card is programmed in order to provide counts N_i on each channel and coincidences between all channels C_{ij} within a tunable time-window of 9 to 20 ns. For this experiment, we measure counts N_0, N_1 and coincidences C_{01}. All data (counts and coincidences) are sent to a computer via a RS232 interface. Acquisitions programs are inspired from those provided by Beck and co-workers [15**?**].

Our interferometer (blue box) is built as symmetric as possible using Crystal Technology $\#3080$ AOMs. The beam waist of the incoming photons from the fiber coupler FC_2 is imaged on AOM_A by lens L_1. Then it is further imaged on AOM_B with the help of lens L_2 in a $2f-2f$ configuration. One output port is then coupled into a 2m-long multimode fiber and directed toward an avalanche photodiode connected to the detection module. The overall length between FC_2 and FC_3 is typically 2 m. For a 9 ns coincidence window the path-length $\mathcal{L}_0$ of the heralding photon (FC_0-APD_0) and $\mathcal{L}_1$ that of the interfering photon (FC_1-APD_1) should be equal to better than 1 m. Assuming a typical $n = 1.5$ refraction index of the fibers we have $\mathcal{L}_0 \approx 1.5 \times 5 = 7.5$ m and $\mathcal{L}_1 \approx 1.5 \times (2+2) + 2 = 8$ m.

The acoustic waves travel in opposite directions in both AOMs so that the frequency shifts almost cancel. The coherence length L_c of our parametric down-conversion source is determined by the spectral width of the filters. L_c is thus on the order of 0.1 mm here. The $2f-2f$ configuration of our interferometer ensures that both AOMs are conjugate, which translates into an equal path length of both arms of the interferometer. The symmetry of the setup makes the path-length difference of second order with respect to small misalignments and displacements and plays probably a key role in the success of the experiment, especially since the coherence of the source is so low.

Alignments are made easy by a separate fiber-coupled 808 nm laser that can be plugged in place of the single photon source at FC_2. At the output side, a flip mirror is lifted up and beams are directed towards conventional linear photodiodes. *Classical* beat notes are then recorded on an oscilloscope (Fig.4 -a).

The two AOMs are driven by a dual output waveform generator, which allows a phase control between the outputs to ensure their phase coherence. They are operated at angular frequencies Ω_A

and Ω_B around their nominal frequency of 70 MHz.

Let us first assume *homodyne operation* $\Omega_A = \Omega_B = \Omega$. We can follow the propagation of the different modes according to the pictorial approach presented in Sec. II and lower part of Fig. 2. The role of the lens L_2 is to deflect the beams towards the second AOM. Due to the symmetry of the setup it reverses the transverse momentum of the photons $\pm q \rightarrow \mp q$. This translates in the exchange of the column of the mode matrix. The effect of the second AOM is then calculated taking into account the opposite direction of the acoustic wave. In practice, light is injected from only one port *e.g.* $E_2 = 0$. The fields at the two output ports are then:

$$\begin{aligned} E_3 &= (r_B^* r_A e^{i\phi_{up}} - t_B t_A^* e^{i\phi_{down}}) E_1^0 e^{-i\omega t}, \\ E_4 &= -(t_B^* r_A e^{i\phi_{up}} + r_B t_A^* e^{i\phi_{down}}) E_1^0 e^{-i(\omega+\Omega)t}, \end{aligned} \tag{5}$$

where explicit time dependance has been added for sake of clarity. $\phi_{up} = \phi_0 + \delta\phi$ and $\phi_{down} = \phi_0 - \delta\phi$ represent the phaseshifts accumulated along the upper and lower arms of the interferometer. Notice that even if the two paths have the same optical length $\mathcal{L}$ the upper one is run along at a slightly higher frequency and present an extra phaseshift $-\Omega\mathcal{L}/c$.

In the ideal case of a perfectly balanced interferometer all reflection and transmission coefficient are real and equal ($|r_{A,B}| = |t_{A,B}| = 1/\sqrt{2}$). The output amplitudes are then $E_3^0 = ie^{i\phi_0} E_1^0 \sin\delta\phi$ and $E_4^0 = -e^{i\phi_0} E_1^0 \cos\delta\phi$. Static complementary fringes are expected at the two output ports when the phase difference $\delta\phi$ is scanned almost as in a conventional Mach-Zenhder. The only difference is the angular frequency shift Ω at output $\#4$ which is not resolved here.

Heterodyne operation is much more interesting. It corresponds to the case where AOMs are driven at different angular frequencies $\Omega_A = \Omega$ and $\Omega_B = \Omega + \delta\Omega$. Our formalism is easily adapted adding an extra $Exp(-i\delta\Omega t)$ to the reflection coefficient r_B of the second AOM. Then, still for a perfectly balanced interferometer, we find:

$$\begin{aligned} E_3^0 &= ie^{i\phi_0'} E_1^0 \sin(\delta\Omega t/2 + \delta\phi), \\ E_4^0 &= -e^{i\phi_0'} E_1^0 \cos(\delta\Omega t/2 + \delta\phi), \end{aligned} \tag{6}$$

with $\phi_0' = \phi_0 + \delta\Omega t/2$. We now expect complementary beat notes at the two output ports.

In a quantum formalism, we would consider the fields as operators ($\hat{E}_3$ and $\hat{E}_4$) and the quantum state would be expressed in the basis of the input modes as $|\psi\rangle = |1\rangle_1 |0\rangle_2$ where $|1\rangle_1$ is a single-photon Fock state in mode 1 and $|0\rangle_2$ is the vacuum state for the mode 2. The expression of output mode $\hat{E}_3$ should include the contribution of the mode $\hat{E}_2$ even if it is in the vacuum state. We can

therefore write:

$$\hat{E}_3 = i\sin(\delta\Omega t/2 + \delta\phi)e^{i\phi'_0}\hat{E}_1 + i\cos(\delta\Omega t/2 + \delta\phi)e^{i\phi'_0}\hat{E}_2 e^{-i\Omega t} \quad (7)$$

The APD measures a photodetected current on mode 3, which is proportionnal to $\langle\psi|\hat{E}_3^\dagger\hat{E}_3|\psi\rangle \propto \sin^2(\delta\Omega t/2 + \delta\phi)$, oscillating at the angular frequency $\delta\Omega$. It is not surprising to find the same result as in the classical treatment: quantum optics textbooks tell us that when we are dealing with linear optics in a counting regime, classical and quantum optics behave similarly.

V. EXPERIMENTAL RESULTS

The experiment can be run in essentially three different ways we now detail successively.

A. Classical beat notes

As shown in Fig. 4, purely classical beat notes are observed when the 808 nm alignment laser is used. We have recorded them for a wide range of frequency differences from mHz up to almost 1 MHz constrained by our photodiodes bandwidth. Using the synchro output of the waveform generator we have also observed the expected temporal shift when scanning the relative phase of the two AOMs. These findings confirm the overall coherence of our setup and, in particular, of AOMs as beam splitters.

B. Classical counting mode

The same kind of signals have been recorded in the count rate of individual photons emanating from the down-conversion source as shown in Fig. 4b. However, even if photons are detected as well separated events, with a mean temporal delay far exceeding the transit time into the interferometer (*i.e.* with less than one photon at a time into the interferometer), these are not considered as true single photon experiments. In such low light experiments, the photon statistics remain classical (poissonian): the delay distribution between two successive photons is a decreasing exponential and thus maximal at zero delay (photon bunching), much like a weak coherent state. See for example [16] for an early experiment of photons heterodyning using low light levels.

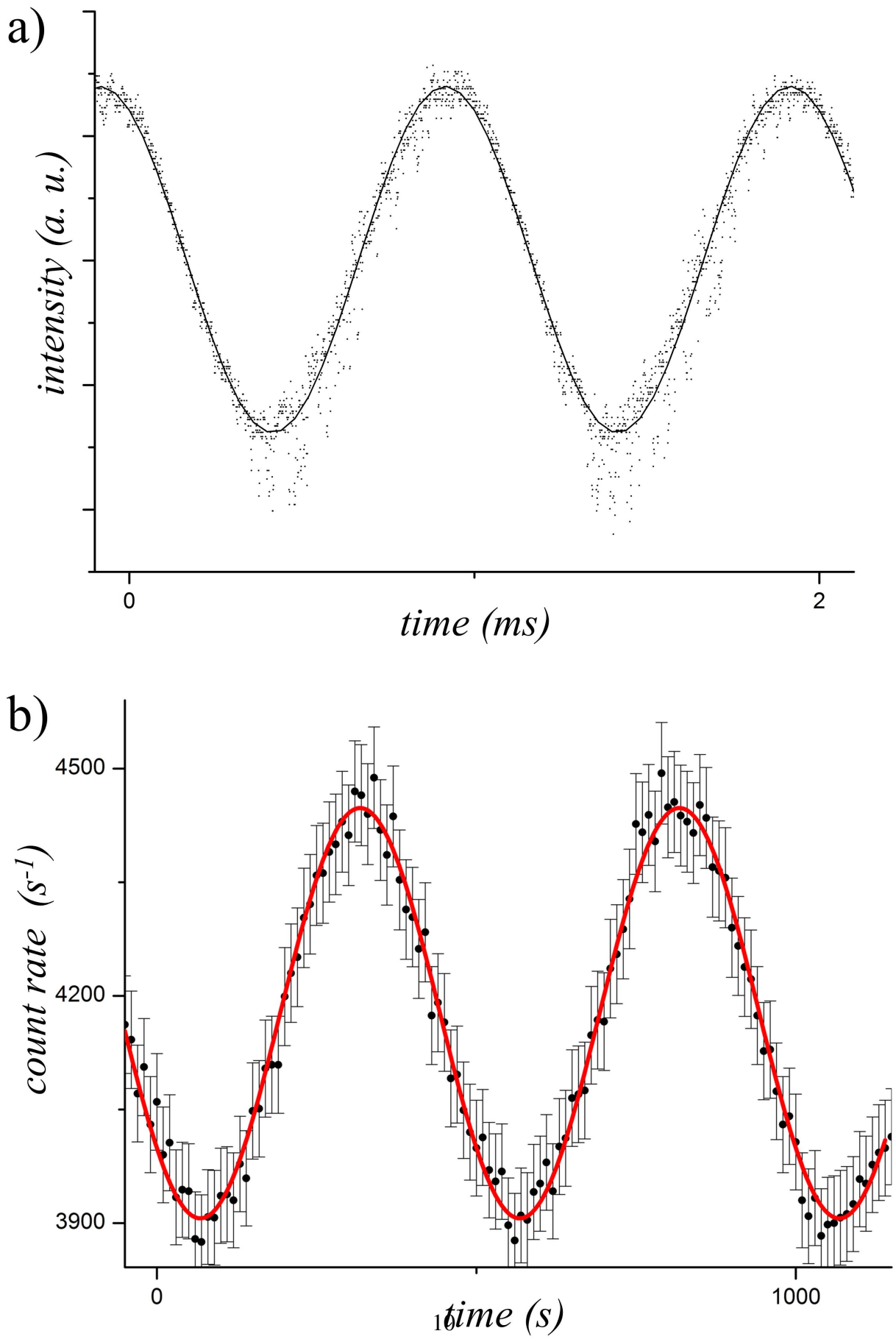

FIG. 4. Classical beat notes. a) Light flux from the 808 nm alignment laser is in the mW range and easily detected on conventional linear photodiodes. AOMs are operated at 1 kHz frequency difference for

C. Single photon beat notes

Fig. 5 shows true single photon beat notes where the parametric down-conversion source is now associated with the FPGA module described earlier to detect coincidences rates between APD_0 and APD_1. The results are obtained when the output photons are detected in coincidence with the heralding photon. Using single quantum events with coincidences counts ensures that we are using true single-photons. It has been carefully checked by Okawa and co-workers that the photons in coincidence diffracted by AOMs have an almost perfect photon anti-bunching behavior ($g^{(2)}(0) = 0$) and that "the single-photon properties remain unchanged after the frequency conversion" in the AOMs [8]. Accidental coincidences (less than 1 per second) can be neglected here given our count rates.

We demonstrated experimentally that beat notes are actually observed at port $\#3$ (see Supplementary Information for a discussion of simultaneous recording of the two output ports). As interaction with AOMs is a coherent process, they persist at the single photon level. It means that output photons are interfering with themselves. More precisely, such photons are elementary excitations of bichromatic field modes [17]. These modes are by essence not eigenstates of the energy and are thus non stationary: their two frequency components produce a beat note at any given position. They are also spatially inhomogeneous as their two wavelengths produce Moiré fringes along the propagation axis at any given time. Orders of magnitude employed in our experiment give rise to somewhat puzzling features: for typical frequency differences of a fraction of a Hertz, the beat notes occur on a few second time scale but the spatial mode period extends over millions of kilometers.

VI. CONCLUSION AND OUTLOOK

An AOM acting as a beam splitter provides both momentum and energy transfert to incoming photons at Bragg angle. With two such beam splitters we realized non stationary single photon states with periodic amplitude in both space and time. Such states are far from the naive picture of a photon being the particle counterpart of a plane wave. Indeed, both electromagnetism and quantum theory are both linear so any superposition of solutions of Maxwell equations is an acceptable field mode to which quantum mechanics associates elementary excitations *i.e.* photons. The striking single photon beat notes observed here are simply the quantum counterpart of a coherent

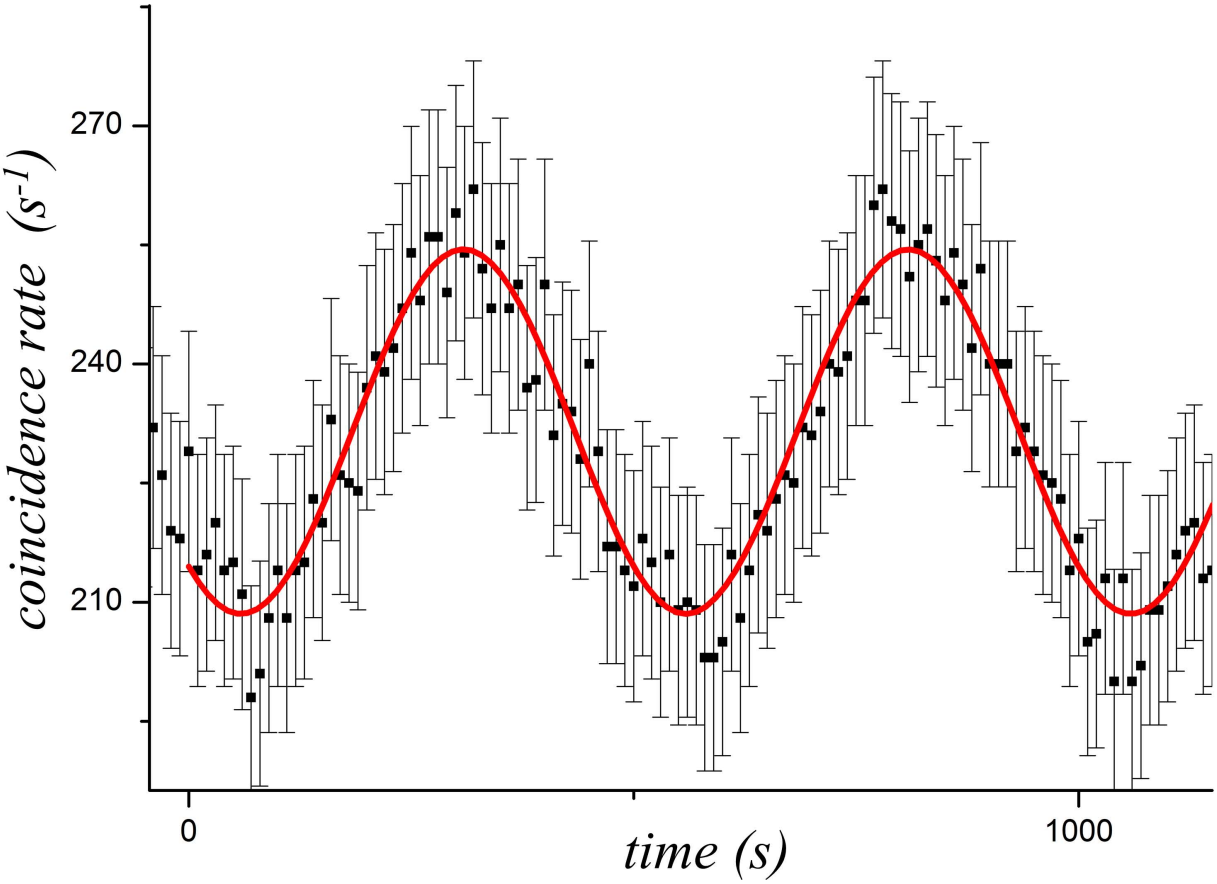

FIG. 5. (Color online) Coincidence rate between the interferometer output (APD_1 see Fig. 4b) and heralding photons recorded on APD_0. Such a coincidence detection ensures, up to negligible random accidental coincidences, that both photons come from the same down-conversion event. A single photon passes through the interferometer exhibiting yet a beat note. From a quantum optics point of view the output field state is an excitation of a superposition of modes of two different frequencies. Such a state has not a definite energy and is thus non-stationary.

bi-chromatic plane wave and if we broaden further the spectrum we may obtain the extreme case of a single photon femtosecond laser pulse. In the early 1960s, Feynman was amazed by the advent of laser technology and envisioned: "Soon, no doubt, someone will be able to demonstrate two sources shining on the wall, in which the beats are so slow that one can see the wall get bright and dark!" [18] We have done a step forward as here, one can see single photons beating on an oscilloscope screen.

This experiment may be considered as a photonic analogue of early days atom interferometry

setups using detuned separated oscillatory fields as beam splitters. These experiments searched for off-diagonal terms of the density matrix of thermal atomic beams [19–21]. Non stationary beam splitters induce energy transfer and thus produce mixing of different energy components in the incoming particles' spectrum. The setup presented here would naturally allow to investigate the same kind of questions about coherence of photon sources.

ACKNOWLEDGMENTS

We gratefully acknowledge Lionel Jacubowiez for fruitful discussions and initiation to experimental quantum optics for pedagogical purposes, Sébastien Tanzilli and Francois Treussart for useful bibliography indications. This project is funded by Programme Investissements d'Avenir under the program ANR-11-IDEX-0002-02, reference ANR-10-LABX- 0037-NEXT.

---

[1] P. G. Merli, G. F. Missiroli, and G. Pozzi, "On the statistical aspect of electron interference phenomena," Am. J. Phys. **44**(3), 306–307 (1976).

[2] R. Bach, D. Pope, S. H. Liou, and H. Batelaan, "Controlled double-slit electron diffraction," New J. Phys. **15**, 033018 (2013).

[3] A. Aspect, P. Grangier, and G. Roger, "Wave particle duality for a single photon," J. of Optics. **20**(3), 119–129 (1989).

[4] V. Jacques, E. Wu, F. Grosshans *et al.*, "Experimental Realization of Wheeler's Delayed-Choice Gedanken Experiment," Science **315**(5814), 966–968 (2007).

[5] D. Dehlinger, and M. W. Mitchell, "Entangled photons, nonlocality, and Bell inequalities in the undergraduate laboratory," Am. J. Phys. **70**(9), 903–910 (2002).

[6] E. J. Galvez, C. H. Holbrow, M. J. Pysher *et al.*, "Interference with correlated photons: Five quantum mechanics experiments for undergraduates," Am. J. Phys. **73**(2), 127–140 (2005).

[7] E. J. Galvez, "Resource Letter SPE-1: Single-Photon Experiments in the Undergraduate Laboratory," Am. J. Phys. **82**(11), 1018–1028 (2014).

[8] Y. Okawa, F. Omura, Y. Yasutake, and S. Fukatsu, "Photon heterodyning," Opt. Exp. **25**(17), 20156–20161 (2017).

[9] L. Olislager, J. Cussey, A.T. Nguyen *et al.*, "Frequency-bin entangled photons," Phys. Rev. A **82**(1),

013804 (2010).

[10] R. Loudon, *The Quantum Theory of Light*, 3rd edition (Oxford University Press, New York, 2000).

[11] A. Zeilinger, "General properties of lossless beam splitters in interferometry," Am. J. Phys. **49**(19), 882–883 (2005).

[12] Y. Park, and K. Cho, "Heterodyne interferometer scheme using a double pass in an acousto-optic modulator," Opt. Lett. **36**(3), 331–333 (2011).

[13] P. G. Kwiat, K. Mattle, H. Weinfurter *et al.*, "New High-Intensity Source of Polarization-Entangled Photon Pairs," Phys. Rev. Lett. **75**(24), 4337–4341 (1995).

[14] J. J. Thorn, M. S. Neel, V. W. Donato *et al.*, "Observing the quantum behavior of light in an undergraduate laboratory," Am. J. Phys. **72**(9), 1210–1219 (2004).

[15] D. Branning, M. Beck, "An FPGA-based module for multiphoton coincidence counting," Proc. SPIE **8375**, 83750F-1–83750F-10 (2012).

[16] C. Davis, "Single-photon optical heterodyning," IEEE J. Quant. Elec. **15**(1), 26–29 (1979).

[17] G. Grynberg, A. Aspect, and C. Fabre, *Introduction to quantum optics: from the semi-classical approach to quantized light*, (Cambridge university press, Cambridge, 2010).

[18] R. P. Feynman, R. B. Leighton, and M. Sands, *The Feynman Lectures on Physics; vol. i*, (Addison-Wesley, Reading Massachusetts, 1964).

[19] E. Smith, A.-A. Dhirani, D. A. Kokorowski *et al.*, "Velocity Rephased Longitudinal Momentum Coherences with Differentially Detuned Separated Oscillatory Fields," Phys. Rev. Lett. **81**(10), 1996–1999 (1998).

[20] R. A. Rubenstein, A.-A. Dhirani, D. A. Kokorowski *et al.*, "Search for Off-Diagonal Density Matrix Elements for Atoms in a Supersonic Beam," Phys. Rev. Lett. **82**(10), 2018–2021 (1999).

[21] K. Rubin, M. Eminyan, F. Perales *et al.*, "Atom interferometer using two Stern-Gerlach magnets," Laser Phys. Lett. **1**(4), 184–193 (2004).